ISSN 0027-1314, Moscow University Chemistry Bulletin, 2008, Vol. 63, No. 5, pp. 250–254. © Allerton Press, Inc., 2008.
Original Russian Text © S.N. Lanin, N.V. Kovaleva, Pham Tien Dung, K.S. Lanina, 2008, published in Vestnik Moskovskogo Universiteta. Khimiya, 2008, No. 5, pp. 300–305.

Adsorption Properties and Surface Chemistry of MgO

S. N. Lanin, N. V. Kovaleva, Pham Tien Dung, and K. S. Lanina

Department of Physical Chemistry
e-mail: SNLanin@phys.chem.msu.ru

Received May 26, 2008

Abstract—The adsorption properties of MgO, which is used as a sorbent and catalyst support, were studied using gas chromatography. The test absorbents used were *n*-alkanes (which show only nonspecific dispersion interactions when physisorbed on any adsorbent) and adsorbates whose molecules are capable of specific interactions with the surface reactive sites of MgO. Adsorption isotherms were measured for $CHCl_3$, CH_3NO_2, CH_3CN, $(CH_3)_2CO$, $CH_3COOC_2H_5$, and $(C_2H_5)_2O$ on MgO at 50–100°C. Differential molar enthalpy changes ($-\Delta H$), equal to molar heats of adsorption, were determined. For polar adsorbates, contributions from dispersive and specific interactions into $-\Delta H$ were determined. The electron-acceptor and electron-donor abilities of the MgO surface were estimated.

DOI: 10.3103/S0027131408050039

Adsorption properties of magnesium oxide have been studied repeatedly [1–8]. Kiselev et al. [2, 3, 8] studied the structure and adsorption properties of magnesium oxide samples prepared by vacuum treatment of large-porosity magnesium hydroxide at 300, 500, 1000, and 1400°C [2] and heating in air at 800, 1000, and 1200°C [8] and those prepared from magnesium carbonate by ignition at 1000°C [3]. The samples prepared from $Mg(OH)_2$ at 300 and 500°C had a bidisperse pore structure: it contained large pores conserved from the initial $Mg(OH)_2$ framework and thin pores (fractures) generated by $Mg(OH)_2$ thermal destruction. The samples prepared at 1000 and 1400°C contained only large pores [3]. The vacuum-calcined magnesium oxide samples had larger surface areas than the samples calcined in air at the same temperature: for magnesium oxide samples calcined in vacuo at 1000°C, the specific surface area was 119 m^2/g; for those calcined in air, it was 14 m^2/g [8]. *n*-Alkanes and aromatic hydrocarbons were used as adsorbates. At relative pressures corresponding to the dominant monolayer coverage, *n*-hexane adsorption on magnesium oxide is higher than benzene adsorption. The adsorption properties of magnesium oxide are strongly affected by its preparation and treatment. For samples calcined at 800 and 1200°C, the heat of benzene adsorption (for the surface coverage $\theta = 0.2$), is 10.4 and 6.4 kcal/mol, respectively [8].

EXPERIMENTAL

Magnesium oxide was purchased from Sigma-Aldrich and had a specific surface area (s) of 6.2 m^2/g determined from thermal nitrogen desorption.

The test adsorbates used were *n*-alkanes C_6–C_9 and their polar derivatives ($CHCl_3$, CH_3NO_2, CH_3CN, $(CH_3)_2CO$, $CH_3COOC_2H_5$, and $(C_2H_5)_2O$). Table 1 lists the characteristics of these adsorbates, where *M* is molecular weight, μ is dipole moment, α is overall

Table 1. Characteristics of test adsorbates (*M*, molecular weight; μ, dipole moment; α, overall molecular polarizability; AN and DN (kcal/mol), electron-donor and electron-acceptor energy characteristics of molecules [9])

Adsorbate	*M*	μ, D	α, Å^3	DN, kJ/mol	AN
n-C_6H_{14}	86.17	0	11.9	0	0
n-C_7H_{16}	100.2	0	13.7	0	0
n-C_8H_{18}	114	0	15.6	0	0
C_6H_6	78	0	10.4	0.418	8.2
$CHCl_3$	119.4	1.15	8.23	0	23
CH_3NO_2	61.0	3.54	7.2	11.297	20.5
CH_3CN	41.1	3.90	5.4	58.994	18.9
$(CH_3)_2CO$	50.18	2.80	6.6	71.128	12.5
$C_2H_5COOCH_3$	88.1	1.78	9	71.546	9.3

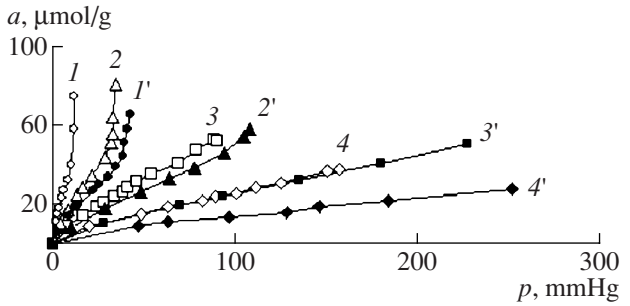

Fig. 1. Adsorption isotherms for *n*-alkanes on MgO at 50 and 75°C: (*1*, *1'*) *n*-C_9H_{20}, (*2*, *2'*) *n*-C_8H_{18}, (*3*, *3'*) *n*-C_7H_{16}, and (*4*, *4'*) *n*-C_6H_{14}.

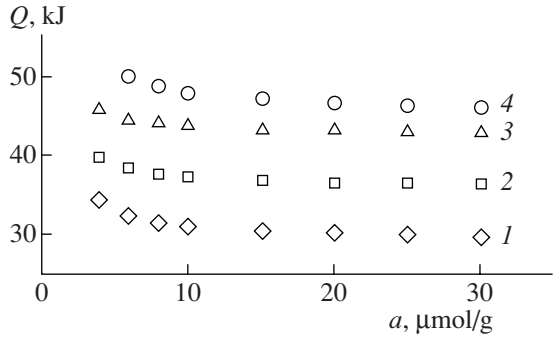

Fig. 2. Isosteric heat of adsorption Q_{st}, kJ/mol, vs. adsorption *a*, μmol/g, on MgO: (*1*) *n*-C_6H_{14}, (*2*) *n*-C_7H_{16}, (*3*) *n*-C_8H_{18}, and (*4*) *n*-C_9H_{20}.

molecular polarizability, and AN and DN are the Gutmann numbers [9, 10] characterizing the ability of these molecules to electron-donor and electron-acceptor interactions.

n-Alkane adsorption on magnesium oxide was studied in a dynamic mode on an LKhM chromatograph equipped with a heat conductance detector. An adsorbent sample (1.1129 g) was placed into a glass column (200 × 2 mm). Before measuring the retention parameters of test adsorbates, the adsorbent was heated for 20 h in the chromatograph column in a carrier gas (He) flow at 150°C. The adsorbate sample volume was 0.2 to 10 μL. The adsorbate retention time was measured at 50, 75, and 100°C. The carrier gas flow rate was 15–25 mL/min. Adsorption isotherms were calculated from developed chromatograms using the Glueckouff method [11].

RESULTS AND DISCUSSION

Interaction of n-Alkanes with the Magnesium Oxide Surface

Figure 1 shows the adsorption isotherms of *n*-alkanes C_6–C_9 measured over the range of the temperatures studied. In their initial segments, the isotherms are convex to the adsorption axis; then, they ascend less strongly to finally acquire the S-shape, which is characteristic of polymolecular adsorption (type II in the system of Brunauer et al. [12]).

For all *n*-alkanes tested, adsorption isotherms become linear within the p/p_s range from 0.05 to 0.6 in the space of the linear form of the BET equation

$$\frac{p/p_s}{a(1-p/p_s)} = \frac{1}{a_m C} + \frac{C-1}{a_m C}\frac{p}{p_s}, \qquad (1)$$

where p and p_s are the equilibrium pressure and saturated vapor pressure of the adsorbate, respectively; a_m is the monolayer capacity, μmol/g; and C is equilibrium constant.

Table 2 lists the values of the constants calculated from this equation.

The same table lists the areas occupied by *n*-alkane molecules in a close-packed monolayer $\omega_{m,1}$ calculated from

$$\omega_m = s/a_m N_A, \qquad (2)$$

where s is the MgO specific surface area and N_A is Avogadro's number.

The $\omega_{m,1}$ values calculated for *n*-heptane and *n*-octane molecular adsorption on MgO are smaller than $\omega_{m,2}$ derived from the density of the liquid on the assumption of a planar arrangement of molecules on the surface [13]. The surface area occupied by an *n*-hexane molecule in a close-packed monolayer is close to the value derived from the density of the liquid with a planar surface coverage by molecules and from the van der Waals molecular sizes for loose packing (ω = 50 Å) [14]. This means that the test adsorbent does not contain micropores commensurate to the size of an *n*-hexane molecule and that the arrangement of *n*-hexane molecules on the surface is planar.

The isosteric heats of *n*-alkane adsorption were determined from

$$Q_{st} = -Rd\ln p/d(1/T). \qquad (3)$$

Interpolated heats of *n*-alkane adsorption on MgO for various adsorption values are displayed in Fig. 2. In the initial adsorption region, Q_{st} slightly decreases because of a small heterogeneity of the surface. Then, starting with $a \geq 10$ μmol/g, the isosteric heats of adsorption remain practically unchanged.

Table 2. Constants a_m and C in the BET equation for *n*-alkanes on MgO (T = 75°C)

Adsorbate	a_m, μmol/g	C	$\omega_{m,1}$, Å^2	$\omega_{m,2}$, Å^2
n-C_6H_{14}	21	9.4	49	51
n-C_7H_{16}	21	10.8	49	54
n-C_8H_{18}	20.1	10.4	51	61

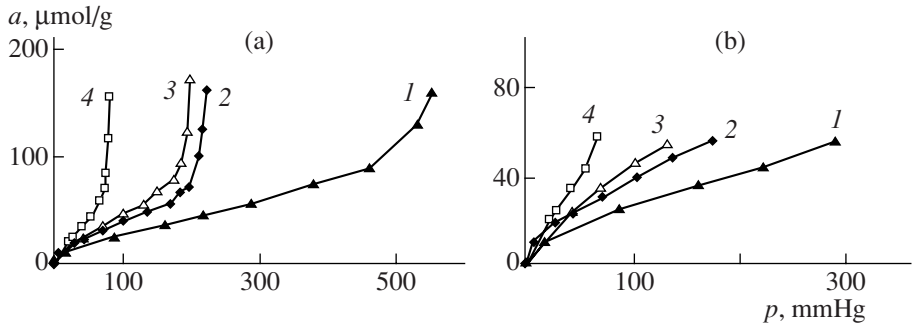

Fig. 3. Adsorption isotherms on MgO for polar adsorbates at 50°C: (a) polymolecular isotherms and (b) initial segments of isotherms for (*1*) $(CH_3)_2CO$, (*2*) $C_3COOC_2H_5$, (*3*) CH_3CN, and (*4*) CH_3NO_2.

Interaction of Polar Adsorbates with the MgO Surface

The S-shaped adsorption isotherms for polar adsorbates shown in Fig. 3 are convex to the adsorption axis in the initial coverage region, indicating strong adsorbate–adsorbent interactions. For p/p_s from 0.1 to 0.7, the adsorption isotherms are well linearized in the space of the linear form of the BET equation. The constants a_m and C of these equations found from the slopes of these lines and the ordinate intercepts are listed in Table 3. The surface areas occupied by adsorbate molecules in a close-packed monolayer, $\omega_{m,i}$ are also listed in Table 3. They were estimated using the BET equation ($\omega_{m,1}$) from the projection of the van der Waals sizes of molecules on the adsorbent surface in close ($\omega_{m,2}$) and loose ($\omega_{m,3}$) molecular packing.

For polar adsorbates, unlike for *n*-alkanes, adsorption drops dramatically for coverages up to approximately $\theta = 0.5$ ($a = 20$ μmol/g) (Fig. 4). This drop signifies the energetic heterogeneity of the surface, that is, the presence of adsorption sites with different activities. These compounds are adsorbed not only via universal dispersion interactions (which increase with molecular polarizability) but also via extra specific, donor–acceptor, or acid–base interactions with the adsorption surface sites of magnesium oxide.

To ascertain the role of particular interactions of polar molecules upon adsorption on MgO, we compared to differential molar changes in the enthalpy of adsorption for *n*-alkanes and polar adsorbates for the identical coverage $\theta = 0.5$. With this surface coverage, the effect of surface heterogeneity is lower, while adsorbate–adsorbent interactions are still not very noticeable. The contributions from dispersive and specific interaction energies into the overall adsorption energy were determined from the heat of adsorption Q as a function of overall molecular polarizability for *n*-alkanes and polar adsorbates. *n*-Alkanes interact with the MgO surface (as with the other adsorbents) only via dispersion interactions, whose energy is proportional to the molecular polarizability. When $\theta = 0.5$, Q_{st} for the adsorption of *n*-alkanes on MgO is described as a func-

Table 3. Constants a_m and C in the BET equation and the surface areas occupied by test adsorbate molecules on the MgO surface

Adsorbate	Temperature, °C	a_m	C	$\omega_{m,1}$	$\omega_{m,2}$	$\omega_{m,3}$
C_6H_6	50	21.2	15.2	48	42	50
	75	22.1	12.2	46	–	–
$CHCl_3$	50	30.3	13.2	34	–	v
	75	34.9	11.4	29	–	–
CH_3NO_2	50	31.9	6.0	32	20	27
	75	30.6	5.8	33	–	–
CH_3CN	50	70.4	6.2	14	20	25
	75	29.9	10.12	34	–	–
$CH_3COOC_2H_5$	50	24	37.8	42	35	48
	75	25.2	33	40	–	–
$(CH_3)_2CO$	50	30.4	19.4	34	26	36
	75	51	6.1	20	–	–

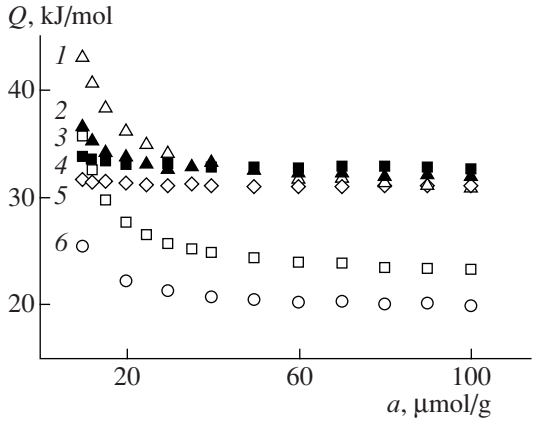

Fig. 4. Isosteric heat of adsorption Q_{st}, kJ/mol, vs. adsorption a, μmol/g, on MgO for (*1*) CH_3CN, (*2*) $CH_3COOC_2H_5$, (*3*) $CHCl_3$, (*4*) CH_3NO_2, (*5*) C_6H_6, and (*6*) $(CH_3)_2CO$.

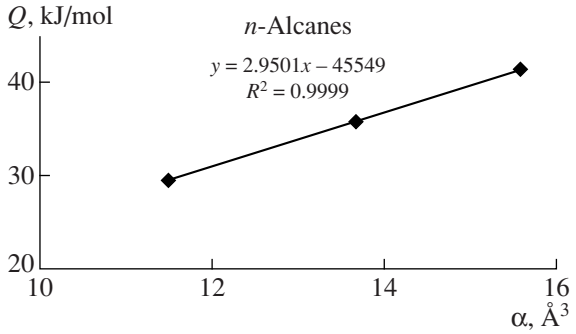

Fig. 5. Isosteric heat of adsorption on MgO Q_{st}, kJ/mol, vs. general polarizability of *n*-alkane molecules.

tion of overall molecular polarizability (a) by the following equation (Fig. 5):

$$Q_{st} = 2.9501\alpha - 4.5549 \text{ [kJ/mol]}. \quad (4)$$

The contribution of the dispersive interaction energy Q_{disp} to the overall energy of adsorption for polar adsorbents was determined from Q_{st} versus polarizability curves for *n*-alkanes (Fig. 5).

The contribution of the specific interaction energy Q_{sp} was determined using Eq. (4) as the difference between the isosteric heat of adsorption Q_{st} of a polar adsorbate and that for a hypothetical *n*-alkane with the same overall polarizability.

Table 4 lists Q_{st}, Q_{disp}, and Q_{sp} for the test *n*-alkanes and polar adsorbates in adsorption on MgO with $\theta = 0.5$.

The specific interaction energy, determined by the electron-donor and electron-acceptor properties of adsorbate molecules and the adsorbent surface, can be expressed as follows [15]:

$$Q_{sp}/AN = K_D + K_A DN/AN, \quad (5)$$

Here, AN and DN are acceptor and donor Gutmann numbers [9, 10] and K_D and K_A are the electron-donor and electron-acceptor characteristics of the surface. Figure 6 illustrates experimental data in the space of this equation.

The values of 1.021 and 0.1305 kJ/mol were, respectively, calculated for the electron-donor (K_D) and electron-acceptor (K_A) characteristics of the MgO surface. From this, the MgO surface has both electron-donor and electron-acceptor sites. The strength and density of these sites on MgO depend on the preparation technique and treatment temperature. The involvement of particular reactive sites in adsorption also depends on the treatment temperature before experiments, the experiment temperature, and the electron-donor and electron-acceptor characteristics of adsorbent molecules.

Table 4. Contributions of the energies of dispersive (Q_{disp}) and specific (Q_{sp}) interactions of test adsorbates to the overall adsorption energy (Q) on MgO (kJ/mol)

Adsorbate	Polarizability, α, Å^3	Q, kJ/mol	Q_{disp}	Q_{sp}	Q_{sp}/Q, %
n-C_6H_{14}	11.9	29.4	29.6	–	–
n-C_7H_{16}	13.7	35.8	35.5	–	–
n-C_8H_{18}	15.6	41.5	41.7	–	–
n-C_9H_{20}	17.9	47	49.2	–	–
C_6H_6	10.4	32.3	24.7	7.6	23.6
CH_3NO_2	7.2	36.8	14.2	22.6	61.4
CH_3CN	5.4	34	8.3	25.7	75.5
$(CH_3)_2CO$	6.6	34	12.3	21.7	64.0
$CH_3COOC_2H_5$	9	36.8	20.1	16.7	45.4
$CHCl_3$	8.23	33	17.6	15.4	46.7

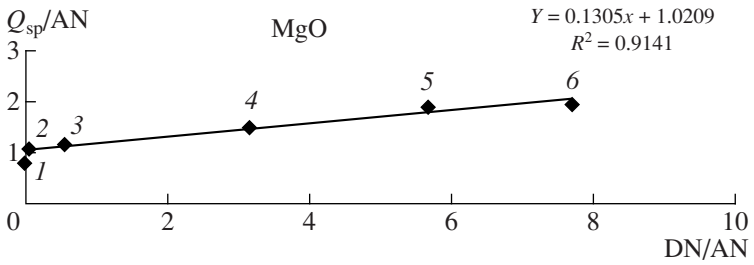

Fig. 6. Determination of KD and KA of the MgO surface: (*1*) $CHCl_3$, (*2*) C_6H_6, (*3*) CH_3CN_2, (*4*) CH_3NO_2, (*5*) $(CH_3)_2CO$, and (*6*) $CH_3COOC_2H_5$.

To conclude, our data imply that the test magnesium sample has not micropores and has a geometrically uniform surface. The adsorption of polar compounds on magnesium oxide involves dispersive and donor-acceptor interactions; the contribution from donor–acceptor interactions to the overall adsorption energy is 23 to 75%.

ACKNOWLEDGMENTS

This work was supported by the Russian Foundation for Basic Research (project nos. 06-03-33131 and 08-03-00824).

REFERENCES

1. Boreskov, G.K., Denisko, V.A., and Borisova, M.S., *Zh. Fiz. Khim.*, 1953, vol. 37, p. 1176.
2. Kiselev, A.V., Neimark, I.E., Poshkus, D.P., and Piontkovskaya, M.A., *Izv. Akad. Nauk SSSR, Ser. Khim.*, 1959, no. 2, p. 232.
3. Kiselev, A.V. and Poshkus, D.P., *Kolloidn. Zh.*, 1959, vol. 21, p. 590.
4. Kiselev, A.V. and Poshkus, D.P., *Kolloidn. Zh.*, 1959, vol. 21, p. 653.
5. Isirikyan, A.A. and Kiselev, A.V., *Zh. Fiz. Khim.*, 1960, vol. 34, p. 2817.
6. Kiselev, A.V. and Poshkus, D.P., *Kolloidn. Zh.*, 1960, vol. 22, p. 25.
7. Kiselev, A.V. and Poshkus, D.P., *Zh. Fiz. Khim.*, 1960, vol. 34, p. 2640.
8. Kiselev, A.V., Nikitin, Yu.S., Petrova, R.S., and Tkhan' Fam Igok, *Kolloidn. Zh.*, 1965, vol. 27, p. 368.
9. Gutmann, V., *Electrochim. Acta*, 1974, vol. 21, p. 661.
10. Gutmann, V., *Coord. Chem. Rev.*, 1991, vol. 18, p. 225.
11. *Eksperimental'nye metody v adsorbtsii i khromatografii* (Experimental Techniues in Adsorption and Chromatography) Nikitinn, Yu.S and Petrova, R.S., Eds., Moscow, 1990.
12. Gregg, S. and Sing, K., *Adsorption, Surface Area, and Porosity*, London, 1967. Translated under the title *Adsorbtsiya, udel'naya poverkhnost', poristost'*, Moscow, 1970.
13. Avgul', N.N., Kiselev, A.V., and Poshkus, D.P., *Adsorbtsiya gazov i parov na odnorodnykh poverkhnostyakh* (Gas and Vapor Adsorption on Uniform Surfaces), Moscow, 1975.
14. Kuznetsov, B.V., *Cand. Sci. (Chem.) Dissertation*, Moscow, 1967.
15. Donnet, J.B. and Park, S., *Carbon*, 1991, Vol. 29, p. 955.